Into the Teeth of the Gale: The Remarkable Advance of a Cold Front at Grand Manan

ROBERT M. CUNNINGHAM
Lincoln, MA 01773

FREDERICK SANDERS
Marblehead, MA 01945

(Manuscript received 7 January 1987, in final form 1 April 1987)

ABSTRACT

The afternoon of 30 December 1962 saw the nearly simultaneous arrival at Grand Manan (an island in the Bay of Fundy) of an intense cold front, accompanied by northwesterly gales and snow, and an intense small cyclonic vortex, producing a mild southeasterly gale. Surprisingly, the cold front arrived first, having advanced over the preceding 9 hours against a geostrophic flow increasing from a few meters per second to about 40 m s^{-1}. The mild air returned for about 2 h as the vortex passed across Grand Manan prior to the final arrival of the mass of cold air. The frontal oscillation was marked by temperature changes from 3°C to −9°C to 3°C to −12°C, within 6 h. There was only a single, strongly defined, low-pressure center.

A simplistic model of the ageostrophic response to geostrophic frontogenetical forcing, neglecting the effects of friction and stratification, shows more than enough ageostrophic flow to account for the observations. Comparison with physically more satisfying models supports the conclusion that this anomalous frontal behavior was the consequence of ageostrophic response to geostrophic forcing acting on an already-intense horizontal temperature gradient, exacerbated by the coincidental approach of an intense cyclone. This comparison also indicates, however, that semigeostrophic theory is not quantitatively reliable when applied to even moderately strong fronts in the real atmosphere.

1. Background

A vacationing meteorologist watching the passing weather without access to VHF or TV tries (and usually can) make a reasonable match between the local observations and an imagined synoptic pattern. One of us (R.M.C.) was trying just that, on a Christmas-week visit to Ingalls Head, New Brunswick, a village on the island of Grand Manan in the Bay of Fundy (Fig. 1). He found, however, that he could *not* imagine a situation that would fit reasonably the sequence of weather events that occurred.

2. The observations

a. A local view

On the morning of 30 December 1962 another wet winter storm system was obviously approaching rapidly, presumably from the SW. The usual sequence was being followed: rapidly falling pressure, an increasing SE wind with snow at first but not for long at this maritime location. It was presumed that on the mainland of Maine and New Brunswick a heavy snow storm would occur. The strong SE breeze became a gale by early afternoon, with moderate rain and rapidly falling pressure by 1500 AST (1900 UTC). Within the next hour the wind changed abruptly to NW, the temperature fell dramatically and the rain turned to snow. It was inferred that the low center had passed nearby and that Ingalls Head might get some of the mainland snowstorm after all, but on the "back side" of the low.

Shortly, however, it became apparent that this neat scenario was not being followed. The pressure, despite the strong NW and then WNW winds, continued to fall very rapidly. Was the low center deepening so rapidly that the pressure would be falling like this after the passage of the low? This seemed unlikely, particularly as the pressure appeared to be falling even more rapidly than when the winds were southeasterly. The possibility that a second low or wave was approaching also seemed unlikely, considering the northwesterly wind direction.

Snow persisted at a moderate rate along with WNW winds until nearly 2000 AST (0000 UTC) when indoor attention was focused on the sound of wind-driven rain hitting the window on the *east* side of the house. Outside, a short time later, it was found that the rain had stopped and a few stars were visible through breaks in the low cloud deck. The wind was strong and relatively mild, once again from the ESE. This wind moderated over the next 2 h, veering toward S. The pressure reached its minimum during this period. These observations suggested the passage of the center of a strong vortex, similar to the eye of a hurricane, as are some-

times evident in satellite views of the center of intense extratropical cyclones.

The major activity during this sudden mild interval was the digging out of many snowbound automobiles—a human activity not typical of hurricane centers. By 2300 AST (0300 UTC) snow was reburying the cars, the wind had veered further to the SW and the temperature had suddenly fallen again. (From local reports it seems that this warm center was not experienced as near as Seal Cove, an island village shown in Fig. 1 to lie 4 miles, or 6 km, west of Ingalls Head.) The observations that were jotted down for this period are shown in Table 1.

b. *The thermograph record*

While spot observations were made at Ingalls Head, a continuous recording of the dramatic changes of temperature was obtained from a thermograph on Kent Island, 6 miles (9 km) to the S, as shown in Fig. 1. This small island is the site of Bowdoin College's Ornithological Research Station. The weather equipment installed and observations made here are the responsibility of one of the authors (R.M.C.). The chart on the thermograph (a Bacharach Tempscribe) had been changed on 26 December and was changed again on 10 January. The instrument is mounted inside a dwelling but the sensor is outside on the north wall, inside a small Stevenson screen. The island is not occupied in winter but the equipment is attended to when bad weather drives the caretaker, a lobster fisherman, into the sheltered island harbor.

The original temperature recording on a circular chart was transcribed on a rectangular plot, shown in Fig. 2, by reading from the original record a sufficient number of points that no significant error was made by connecting them with straight line segments, and by correcting these values slightly on the basis of previous comparisons with a standard thermometer. No correction was made for possible timing errors. There is close correspondence between this record and the temperature behavior indicated for Ingalls Head on the basis of the hourly observations, also seen in Fig. 2. Note that at Ingalls Head the initial plunge of temperature occurred about an hour earlier and the final one about an hour later. These time differences imply arrival of the first surge of the cold air from the north and the second from the south. In view of the wind observations at Ingalls Head, these implications are consistent with the hardly disputable assumption that the temperature changes were the result of advection.

c. *A barograph trace*

The nearest barograph trace was obtained from the National Weather Service office at Eastport (EPO). This station, as seen in Fig. 1, lies about 21 miles (32 km) northwest of Ingalls Head. A detailed transcription of the trace, with the five available surface observations from EPO (including data from a maximum–minimum thermometer), appears in Fig. 3. It is likely that a cold front was passing the station at 1800 UTC, when the wind was observed to have shifted to northwesterly but the temperature had fallen little. Except for hesitations in the rate of pressure fall around 1600 and 2000 UTC, there is little evidence of an effect of the front, as was the case at Ingalls Head. The brief warm core observed at the latter site evidently did not reach EPO with comparable strength, to judge from the maximum temperature of only 22°F (−5.6°C) during the period from 0600 to 1200 UTC 31 December, when the low center passed close to the station.

3. The synoptic situation

The synoptic context in which these remarkable events occurred is illustrated in Fig. 4. The flow at 1200 UTC 30 December was highly meridional. At the surface, a frontal trough at the eastern boundary of a mass of bitterly cold air lay close to long 70°W from the

TABLE 1. Weather observations at Ingalls Head for 30 December 1962.

Time			Wind		Temp.	
AST	UTC	Weather	(mph)*		(°F)*	Remarks
0800	1200	Light snow and rain	SE	25	35	
1100	1500	Light rain	ESE	30	36	
1400	1800	Light rain	SE	40	37	
1500	1900	Mod. rain	SE	30	37	
1600	2000	Heavy snow	NW	30	20	Pressure continues to fall rapidly.
1700	2100	Heavy snow	WNW	25	15	
1800	2200	Mod. snow	WNW	30	15	
1900	2300	Mod. snow	WNW	20	18	
2000	0000	Broken low clouds	ESE	30	38	Rain just before 8 p.m.
2100	0100	Broken low clouds	SE	20	38	
2200	0200	Overcast	S	20?	35	Weather changing rapidly.
2300	0300	Light snow	SW	20	12	Pressure rising rapidly.

* 1 mph = 0.447 m s^{-1}, °F = 9/5°C + 32.

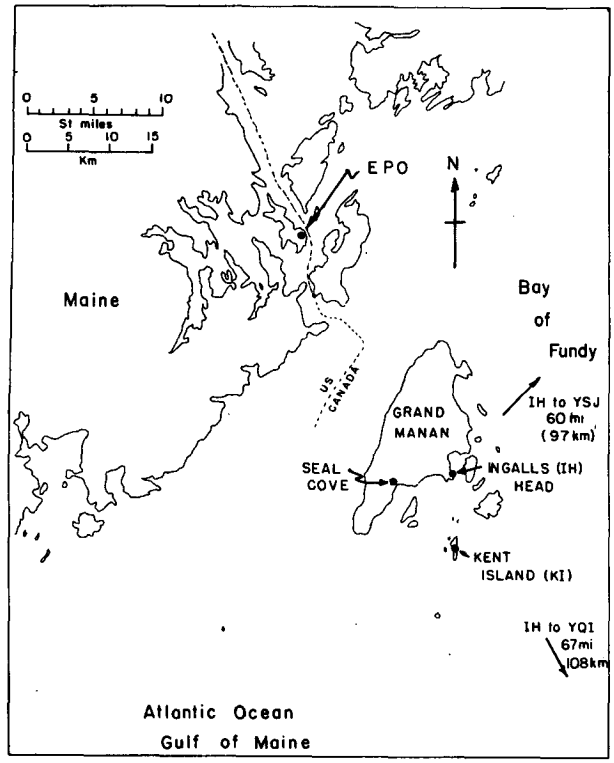

FIG. 1. Map of Grand Manan and vicinity, showing location of several places mentioned in the text.

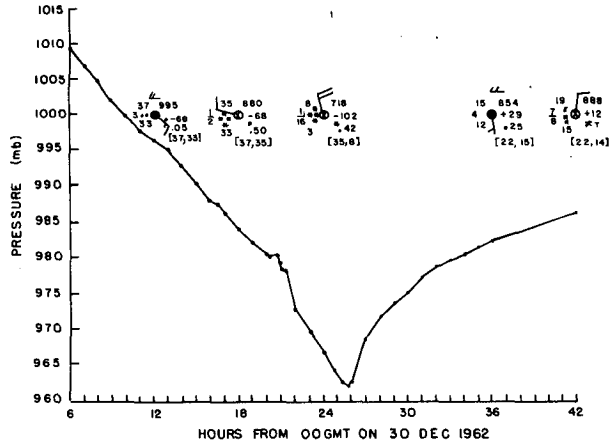

FIG. 3. Time trace of pressure at EPO, with available surface observations plotted in the conventional manner, except that the maximum and minimum temperatures in the preceding 6 h appear in brackets below each observation. Temperatures are in °F (°F = 9°C/5 + 32), and visibilities are in miles (1 mile = 1.6 km).

subtropics to the polar regions. Maximum temperature differences over 100 km within the baroclinic zone were approximately 10°C except over the westernmost Atlantic, where they were reduced, presumably by strong heating of the colder air. At upper levels, strong meridional flow was evident on both sides of a trough which tilted to the west with elevation, lying at 500 mb some 500 km to the west of the surface trough. The temperature contrast associated with the surface frontal zone was evident at least through the 700-mb level, weakening with elevation. Strong cold advection was occurring at the 500-mb trough line, indicating intensification of the system.

Of particular interest within the surface frontal trough was the small, growing, vortex near 38°N, 68°W, already intense enough to produce 25–30 m s^{-1} winds within 200 km from the center. This explosively-deepening cyclone (about 25 mb in the preceding 18 h) was occurring within a favored region, according to data presented by Roebber (1984). The 1200 UTC distributions of wind, pressure and temperature around this storm and along the frontal trough between lat 35°N and 50°N are shown in Fig. 5a. Note that the WNW wind at ACK, a site with no prominent orographic obstacles, was blowing nearly perpendicular to the isobars at 16 m s^{-1}. (Locations are shown in Fig. 6 as well as in Fig. 1.) The surge of cold air had evidently resulted in a crowding of the isotherms along the frontal zone here, as there was a difference of 12°C between this station and the location of the ship to the east-southeast, where a SSE wind was reported. A suggestion of a similar but weaker surge in Maine was indicated by the ageostrophic WNW winds near 10 m s^{-1} at MLT and OLD and a slight eastward bulging of the isotherms there.

During the following 10 h the deepening vortex tracked at 21 m s^{-1} along a cyclonically-curved track, being near 41°N, 65°W at 1800 UTC (Fig. 5b) and lying about 100 km southeast of YQI at 2100 UTC (Fig. 5c). During this time the forward surge of cold air in southern Maine became more and more pronounced, arriving at Grand Manan, as we have seen, before the cyclone. The temperature contrast at this

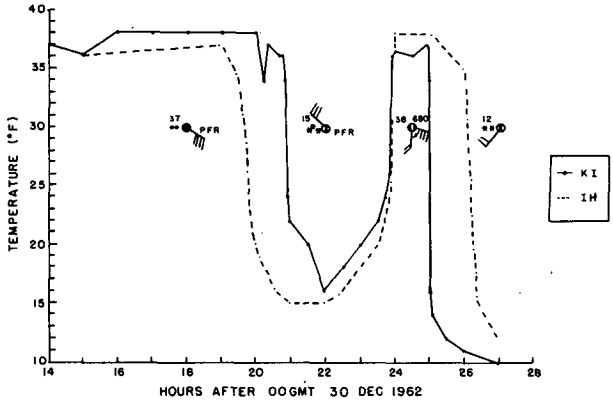

FIG. 2. Time trace of temperature at Kent Island (solid) and Ingalls Head (dashed), with selected observations from the latter site, plotted in the conventional manner. Temperature scale and plotted temperatures are in °F (°F = 9°C/5 + 32).

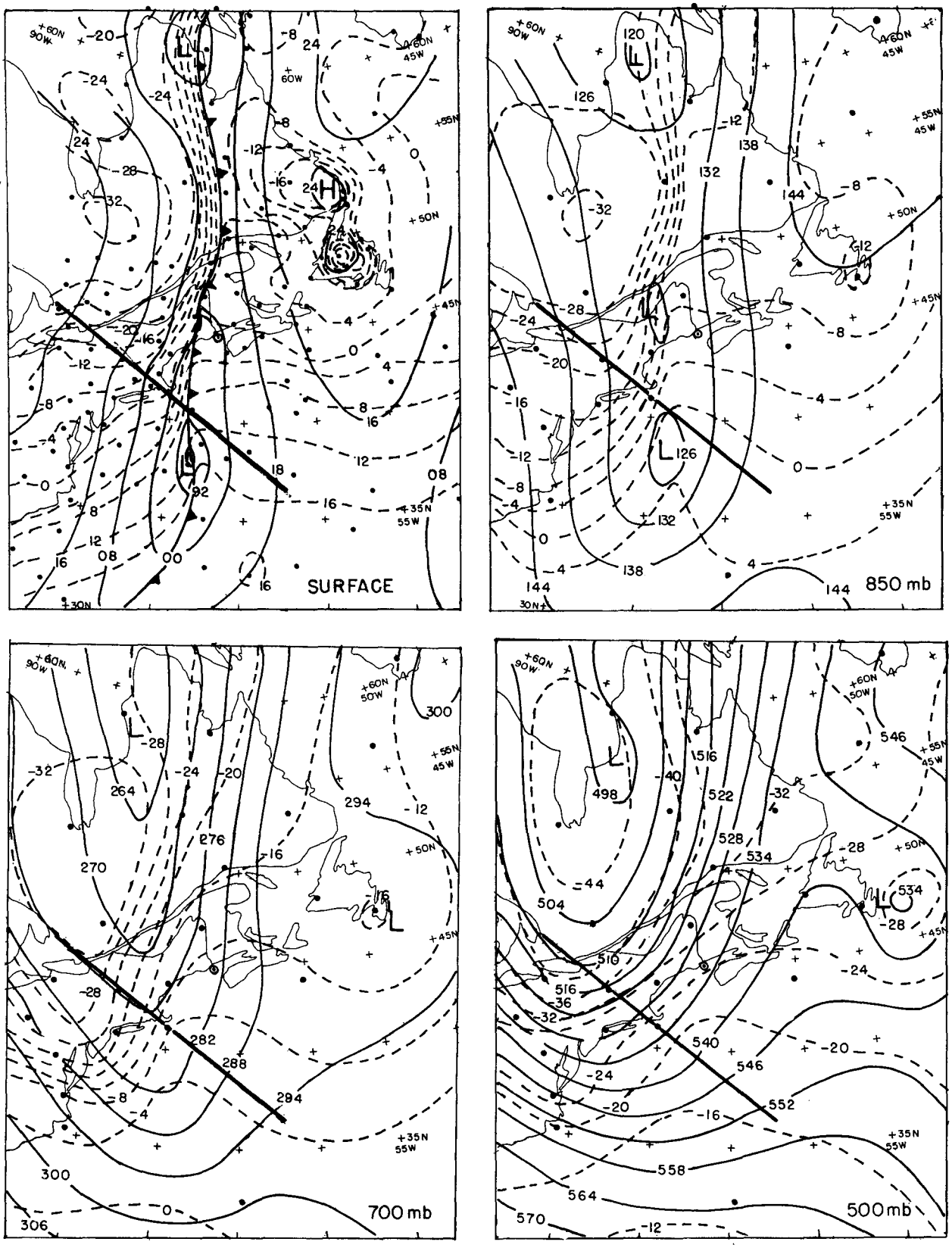

FIG. 4. (a) Surface analysis for 1200 UTC 30 December 1962. Solid lines are isobars of sea level pressure at intervals of 8 mb. Dashed lines are isotherm of surface temperature at intervals of 4°C. The surface front is shown in the conventional manner. (b) 850-mb, (c) 700-mb and (d) 500-mb analyses for the same time and with the same convention, except that the solid lines are height contours at intervals of 6 dam. Dots show position of observations used in the analysis. The circled dot shows the location of Grand Manan. The heavy solid line shows the position of the vertical cross section in Fig. 11.

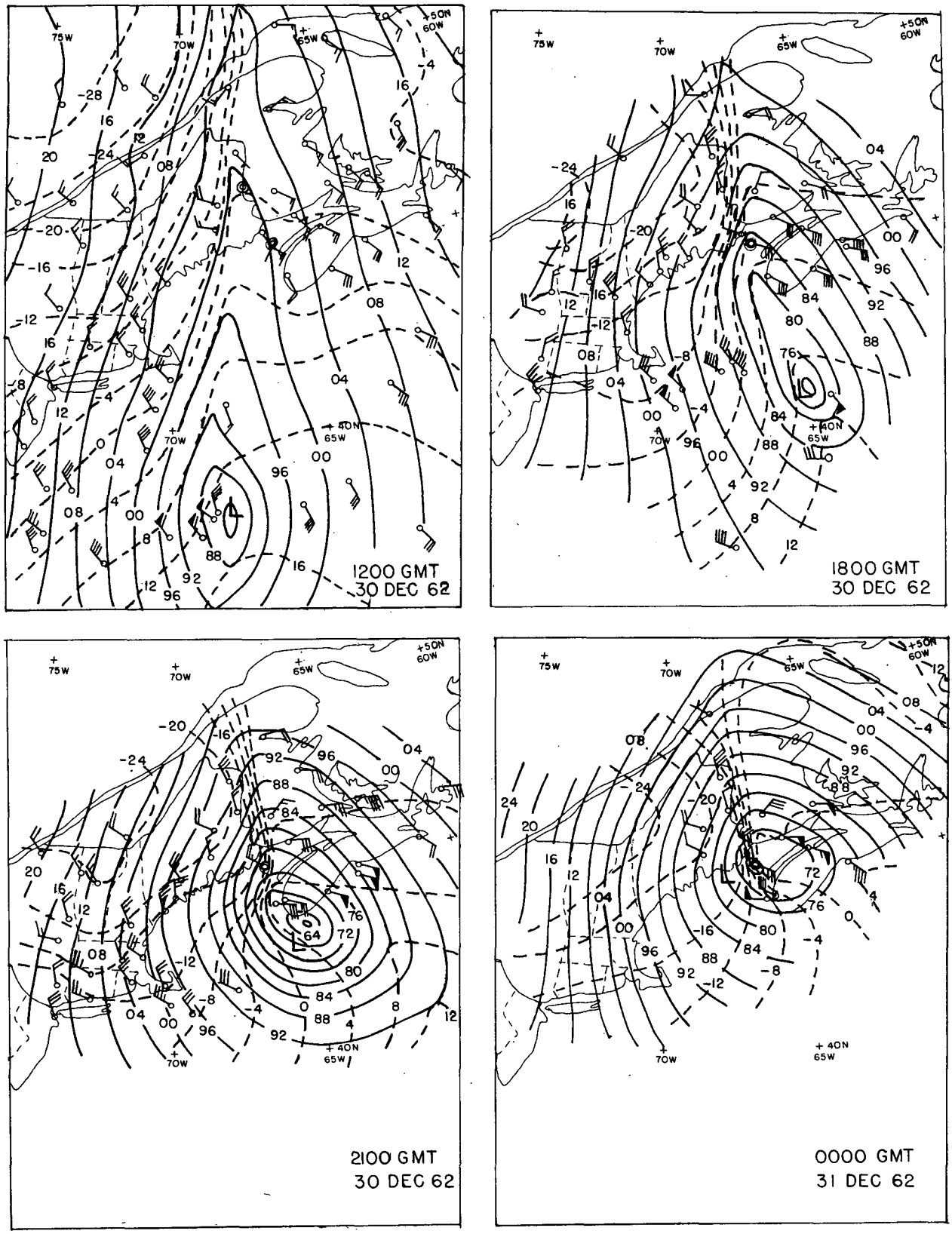

FIG. 5. Detailed surface maps, with isobars (solid) at intervals of 4 mb and isotherms (dashed) at intervals of 4°C, for the times indicated, on 30 and 31 December 1962. Surface winds are plotted in the conventional manner. The circled station is Grand Manan.

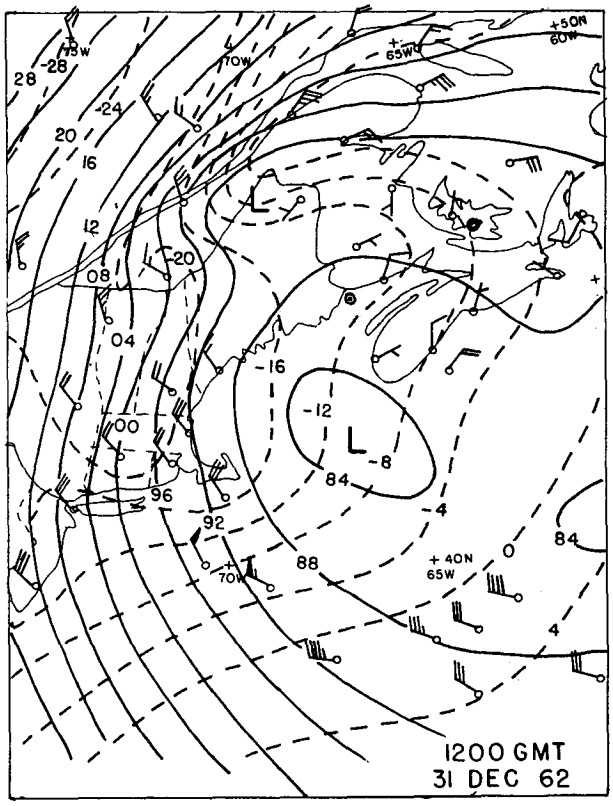

FIG. 5. (*Continued*)

time had collapsed to a virtual discontinuity, as was evident from the thermograph record at Kent Island.

The next hour saw the pressure at YQI fall to a minimum (on the hourly observations) of 959.8 mb, with a maximum temperature of 5.6°C and gusts to near hurricane force from the ESE. One hour later still the vortex had passed and the cold air arrived: pressure 964.3 mb, temperature −3.9°C and NW gusts to 36 m s^{-1}. The strongest winds here, and the most rapid pressure changes here and at EPO (see Fig. 1) occurred very close to the center.

By 0000 UTC on the 31st (Fig. 5d), the vortex, now slowing and filling rapidly, was crossing Grand Manan, as recounted above, enroute to EPO where the pressure minimum was observed between 0100 and 0200 UTC. Subsequently, the cyclone moved northwestward into Maine and then circled counterclockwise back into the Gulf of Maine, becoming part of a belt of low pressure which had developed in the cold air south of Nova Scotia. By 1200 UTC a weak low is shown in Fig. 5e west-northwest of CAR on the old front, which had continued moving northward. By this time there was no trace of the marked temperature discontinuity in the vicinity of Grand Manan, shown in Figs. 5c and 5d, but strong contrast, and perhaps a new discontinuity, appeared along the front in the St. Lawrence Valley, between YBG and YYY.

The situation at upper levels could not be analyzed satisfactorily at 0000 UTC on the 31st, because crucial soundings at CAR and WSA (44°N, 60°W) were not available. The rough analyses lacking these observations, however, showed that a cutoff cyclone center at 500 mb had formed on the New England coast between PWM and ACK and that the flow aloft over the surface vortex was southeasterly. Thus its motion toward the northwest, while unusual, was readily explainable.

The aspect of the case which seems most mysterious is the continued eastward creep of the surface front and accompanying cold air in Maine and New Brunswick in the face of contrary geostrophic flow. The situation is illustrated specifically in Fig. 6, where we see that the approach of the vortex from the southeast (and the enlargement of its closed circulation) produced increasing westward geostrophic components along the frontal zone reaching 30–40 m s^{-1} by 2100 UTC, while the zone itself continued eastward at 3–4 m s^{-1}.

4. Frontogenesis and ageostrophic motion

The explanation is to be sought in the ageostrophic component of motion normal to the baroclinic zone. Our present understanding, based on the ideas of Sawyer (1956), Eliassen (1959), Hoskins and Bretherton (1972) and others, is that the geostrophic advection of

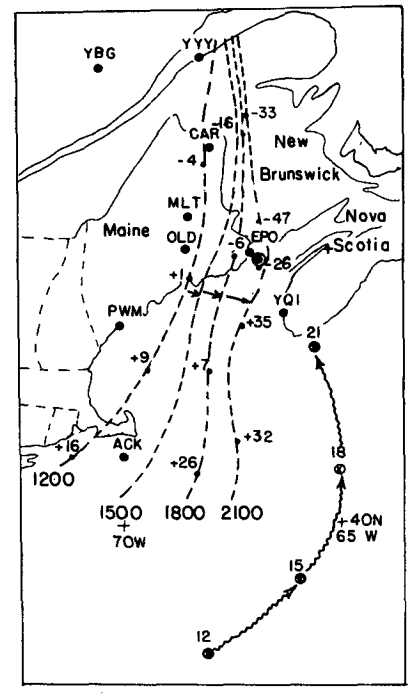

FIG. 6. Isochrones (UTC) of the −4°C isotherm (dashed) and path of the cyclone (wriggly arrows) with positions shown at indicated GMTs. Small dots show selected points with measurements of u_g in m s^{-1} at the indicated times. Place names and station locations added. Large circled dots show position of Grand Manan.

temperature is the prime mover. If it is arranged so as to increase the strength of the horizontal temperature gradient, then the tendency of the atmosphere to remain in thermal-wind balance requires a simultaneous increase of the component of vertical wind shear along the isotherms. As shown by Thorpe (1985), it then follows from the equation of frictionless horizontal motion that there must be a vertical shear of the *ageostrophic* component of wind normal to the isotherms. This shear is most easily realized if there is ageostrophic flow from cold to warm air near the ground and from warm to cold at the top of the layer in which the frontogenetical forcing is present. If this situation exists only for some finite distance away normal to the developing front, then there will be a vertical variation of the horizontal divergence, such that the warmer air will rise and the colder air will sink.

The accompanying adiabatic temperature changes will operate against the strengthening of horizontal temperature gradient being driven by the geostrophic flow, so as to moderate the need for the ageostrophic circulation in the first place, but the requisite circulation can be computed for any given set of circumstances. At the ground, of course, the vertical motion and the adiabatic temperature changes will vanish, so that the frontogenesis proceeds unopposed. Finally, the advection of temperature by the ageostrophic flow itself will exacerbate the situation near the ground at the warm edge of the zone of contrast, leading to development of a virtual discontinuity there.

The consequences described in this account resemble closely what happened in this case, as illustrated by Fig. 5. We will now try to see whether the geostrophic frontogenesis was strong enough to account for the observed ageostrophic motion of the front. The conventional way to measure this advective frontogenetical effect is to determine the total deformation field and to compare the orientation of the axis of dilatation and of the isotherms. A more economical way is to use natural coordinates, with the n-axis normal to the isotherm (toward the warmer air) at each point and the s-axis parallel to it. For convenience we denote the components along these axes u and v, respectively. Then the strengthening of the gradient due to geostrophic advection is given by

$$\frac{\partial}{\partial t}\frac{\partial T}{\partial n} = -\frac{\partial u_g}{\partial n}\frac{\partial T}{\partial n}, \tag{1}$$

which contains the tacit assumption that there is no adiabatic heating or cooling, as would be the case, for example, if the static stability were zero.

The rate of increase of vertical wind shear may be expressed by

$$\frac{\partial}{\partial p}\frac{\partial v}{\partial t} = \frac{\partial}{\partial t}\frac{\partial v_g}{\partial p} = -\frac{R}{fp}\frac{\partial}{\partial t}\frac{\partial T}{\partial n}. \tag{2}$$

The vertical shear of the acceleration, neglecting friction and on the assumption that there is no advection of velocity, is given by

$$\frac{\partial}{\partial p}\frac{\partial v}{\partial t} = \frac{\partial}{\partial p}\frac{dv}{dt} = -\frac{f\partial u_{ag}}{\partial p}. \tag{3}$$

Combining Eqs. (1), (2) and (3), we find that

$$\frac{\partial u_{ag}}{\partial p} = \frac{R}{f^2 p}\left(-\frac{\partial u_g}{\partial n}\frac{\partial T}{\partial n}\right). \tag{4}$$

We then introduce finite differences and assume for simplicity a linear variation of u_{ag} with pressure over the layer from near the surface at 1000 mb to, say, 700 mb, with $u_{ag}\,(1000) = -u_{ag}\,(700)$. The appropriate expression for u_{ag} near the surface is then

$$u_{ag}\,(1000) = \frac{R}{2f^2}(300/850)\left(-\frac{\partial u_g}{\partial n}\frac{\partial T}{\partial n}\right). \tag{5}$$

To obtain a working formula, we measure differences of u_g and T over distances of 100 km normal to the isotherm, and we take $R = 287\ \mathrm{m^2\,s^{-2}\,K^{-1}}$ and $f = 10^{-4}\ \mathrm{s^{-1}}$. Then, at 1000 mb,

$$u_{ag}\,(\mathrm{m\ s^{-1}}) = -0.5\delta u_g\,(\mathrm{m\ s^{-1}})\delta T\,(\mathrm{K}). \tag{6}$$

5. Results for this case

a. The simple model

Measurements of u_g were made by estimating the difference of height of constant-pressure surfaces over distances of 222 km along each isotherm for selected portions of the charts shown in Figs. 4 and 5. For this purpose, an increment of 8 mb in sea level pressure was regarded as the equivalent of 6 dam in 1000-mb height. Then the values of $\delta u_g \delta T$ required by formula (6) were obtained at a sufficient number of points to outline the areas of maximum frontogenetical forcing.

Results appear in Fig. 7 for the surface at the times shown in Fig. 5 and in Fig. 8 for the other levels shown in Fig. 4. It should be noted that the formula almost certainly yields a substantial overestimate of the vigor of the ageostrophic circulation, because of the neglect of friction and of stratification, especially in the relatively stable cold air mass. To assume that the value measured at the surface represents the entire layer up to the 700-mb level is ill-advised (as can be confirmed by the fields shown in Fig. 8), since the horizontal temperature gradient in this case had maximum strength at the surface and weakened substantially with elevation.

With these reservations in mind, we note that at 1200 UTC on the 30th (Fig. 7a), a narrow zone of strong forcing scarcely 100 km wide followed the frontal band of strong temperature contrast from just northwest of the cyclone to south-central Maine. The peak value of $\delta u_g \delta T$ about 100 km southeast of ACK

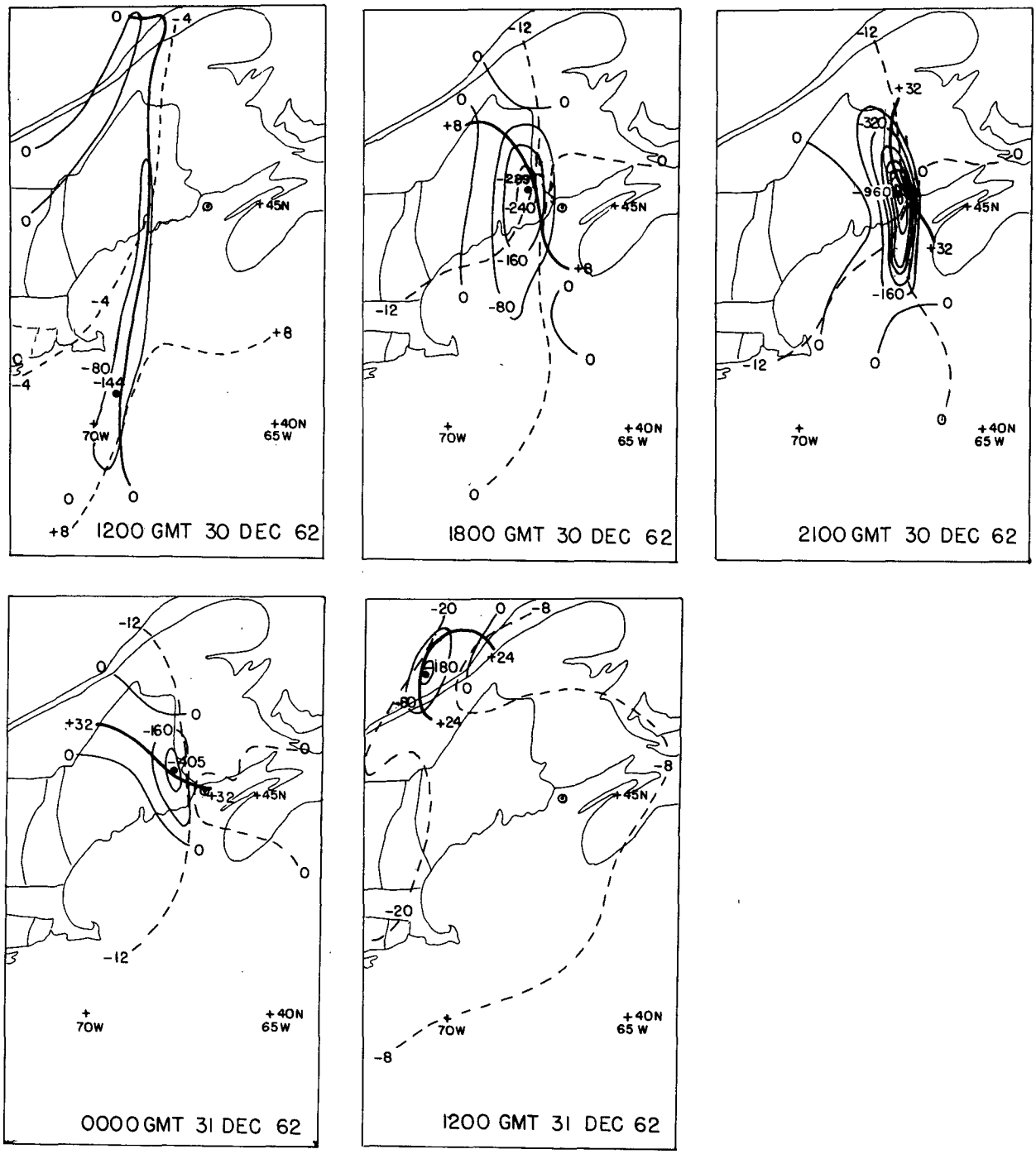

FIG. 7. Selected isopleths of geostrophic frontogenesis rate (thin solid) with the maximum values shown by large dots, in units of K (100 km)$^{-1}$ (10^5 s)$^{-1}$, for indicated times. Selected isotherms are shown by dashed lines, labeled in °C, and a representative isopleth of u_g in the frontogenetical zone is indicated by a heavy solid line. Larger values lie to the east of the heavy line. See text. Circled dot shows position of Grand Manan.

was -144 m s^{-1} K, implying from (6) the overly ample value of 72 m s^{-1}. Six hours later (Fig. 7b), the peak values of this product had moved northeastward about the same distance as had the cyclonic vortex. The peak value had grown to -289 in eastern Maine. Pronounced W to NW winds were crossing the isobars at a large angle in this region and the eastward bulge of the isotherms was becoming more pronounced.

After another 3 hours (Fig. 7c) enormous changes had occurred. The front had passed Kent Island as a virtual discontinuity, as described above, and a NW wind of about 13 m s^{-1} was blowing at Ingalls Head indicating u_{ag} near 40 m s^{-1}. The peak value of the frontogenetical product had risen to −972, just north of EPO where u_{ag} was probably close to 50 m s^{-1} along the edge of the cold in western New Brunswick. Even these spectacular values were nearly an order of magnitude smaller than indicated by the simplistic Eq. (6), but the qualitative coincidence of the strong forcing and the strong response is striking.

The slight retreat of the cold air at 0000 UTC at the Kent Island site and on Grand Manan cannot be convincingly explained. We may point out, however, that the frontogenetical forcing was weakening markedly (Fig. 7d), while the vigor of the geostrophic circulation was largely unabated despite marked filling of the small central vortex after it passed YQI. Evidently the balance immediately in advance of the vortex was tipped just slightly in favor of the geostrophic advection of warm air.

By 1200 UTC on the 31st, Fig. 7e shows no trace of discontinuity or strong frontogenetical forcing in the area. In the St. Lawrence Valley northwest of the remnant cyclone, however, there was a region of prominent temperature contrast and forcing, probably representing propagation of the same feature seen earlier. It appears relatively weak, but the available data preclude an attempt to determine whether a virtual discontinuity exists.

The vertical structure of the baroclinic zone and the frontogenetical forcing could be satisfactorily determined only at 1200 UTC on the 30th. At 850 mb, Fig. 8a shows two centers of forcing, one associated with each of two lows in the height field. The maximum product of $\delta u_g \delta T$ in the southern one, of main interest, was −72, half the value seen at the surface in Fig. 7a. The dual structure persists at 700 mb (Fig. 8b) and perhaps at 500 mb (Fig. 8c), weakening further with elevation.

Two relevant soundings are available, for PWM and ACK, both within the zone of frontogenesis but west of the maximum values (cf. Fig. 7a). They appear in Fig. 9, and hodograms are shown in Fig. 10. At both sites there was a well-mixed boundary layer, somewhat deeper at PWM than at ACK. This was capped by a deep stable layer with no clear upper boundary. Within this frontal zone maximum vertical wind shear was observed between 2–3 km at PWM and between 1–2 km at ACK. At the former station dry air intruded in the layer between 700 and 400 mb, between cloudy air below and a reported cirrus overcast above. At ACK snow of moderate intensity was observed, and the air was no doubt saturated to considerable depth.

The important point to be noted in the hodograms is that the observed wind shear at both stations, from the maximum at the top of the boundary layer to 4 km, is rotated decidedly counterclockwise from the direction of the thermal wind, as indicated by the direction of the isotherms at the standard pressure levels. This is consistent with the argument presented earlier, that the ageostrophic wind should be toward the warmer air near the surface and toward the colder air aloft. The near-surface ageostrophic wind, u_{ag}, at the top of the boundary layer appears to be a few m s^{-1} at PWM and at least 10 m s^{-1} at ACK.

b. *Other calculations*

The semigeostrophic model of Emanuel (1985) contains the important effects, neglected in ours, of adiabatic warming and cooling and of advection of the geostrophic momentum by the three-dimensional ageostrophic circulation. To see what effects these processes might have, we prepared a vertical cross section for 1200 UTC of the 30th, along a line through ACK approximately normal to the mean tropospheric isotherms, shown in Fig. 8. The result appears in Fig. 11. The sloping frontal zone is clearly evident in the fields of potential temperature and of saturation equivalent-potential temperature (the relevant thermodynamic quantity where the air column is deeply saturated, as is no doubt the case near ACK).

By comparing the slopes of the isopleths of M_g, the geostrophic momentum in the direction normal to the section, with the slopes of isopleths of the appropriate thermodynamical quantity, we see that the symmetric stability relevant to semigeostrophic theory is near zero in the warm air adjacent to the frontal zone up to about 350 mb. The apparent symmetric instability in the vicinity of ACK between 600 and 350 mb may be spurious, since the actual wind speeds and shears in this region are subgeostrophic. In these conditions, Sanders (1986) has shown that the geostrophic approximation underestimates the symmetric stability. Within the colder air there is pronounced stability; and farther to the southeast the warmer air may be unstable for upright convection up to near the 700-mb level but is otherwise symmetrically stable.

The geostrophic confluence, forcing frontogenesis, is shown in Fig. 11 as the change in u_g over distances of 200 km along the section line. It is seen to be strongly concentrated on a relatively small scale near the surface. Aloft it is much broader and weaker, although the gradient of the geostrophic momentum along the section line remains relatively constant. This vertical variation in structure is not contained in Emanuel's (1985) model.

In this model, the forcing, Q, assumed constant in the vertical, is proportional to $(\delta u_g/\delta M_g)(\delta\theta/\delta M_g)$. From Fig. 11, the maximum values of this product are estimated to be −0.46 m s^{-1} (K) at 1000 mb and −0.08 at 500 mb. Having no better choice, we make calcu-

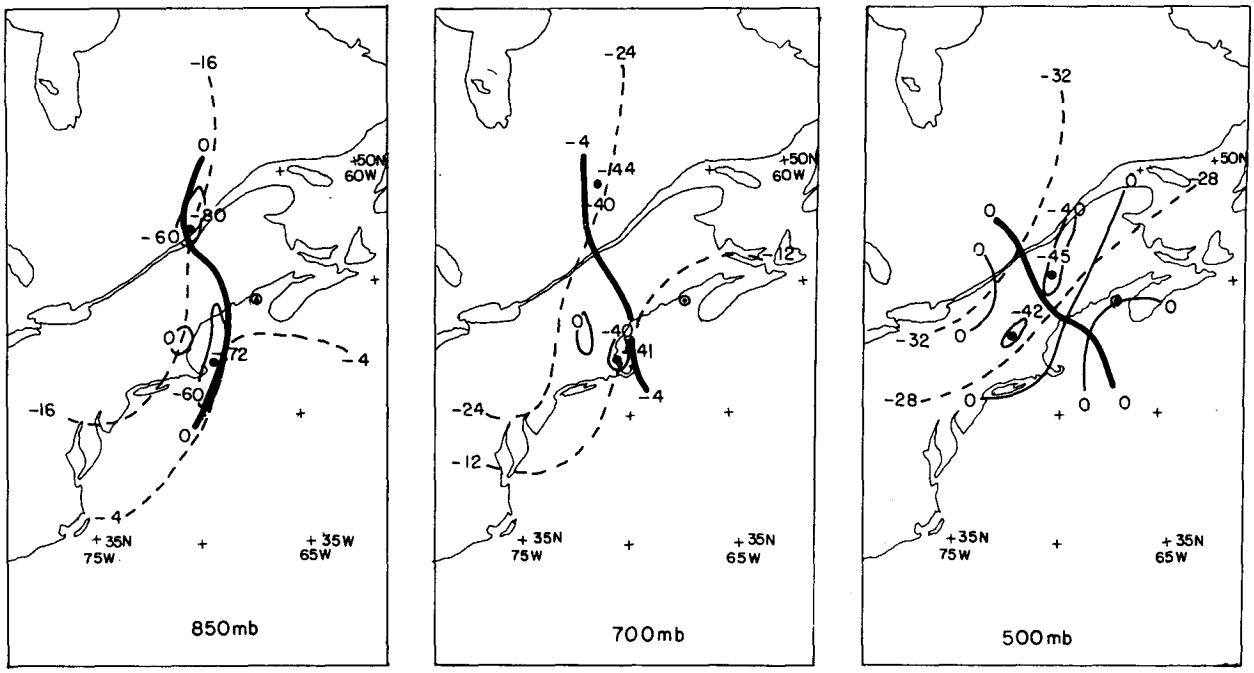

FIG. 8. Geostrophic frontogenesis at indicated upper levels at 1200 UTC 30 December 1962. Format same as in Fig. 7.

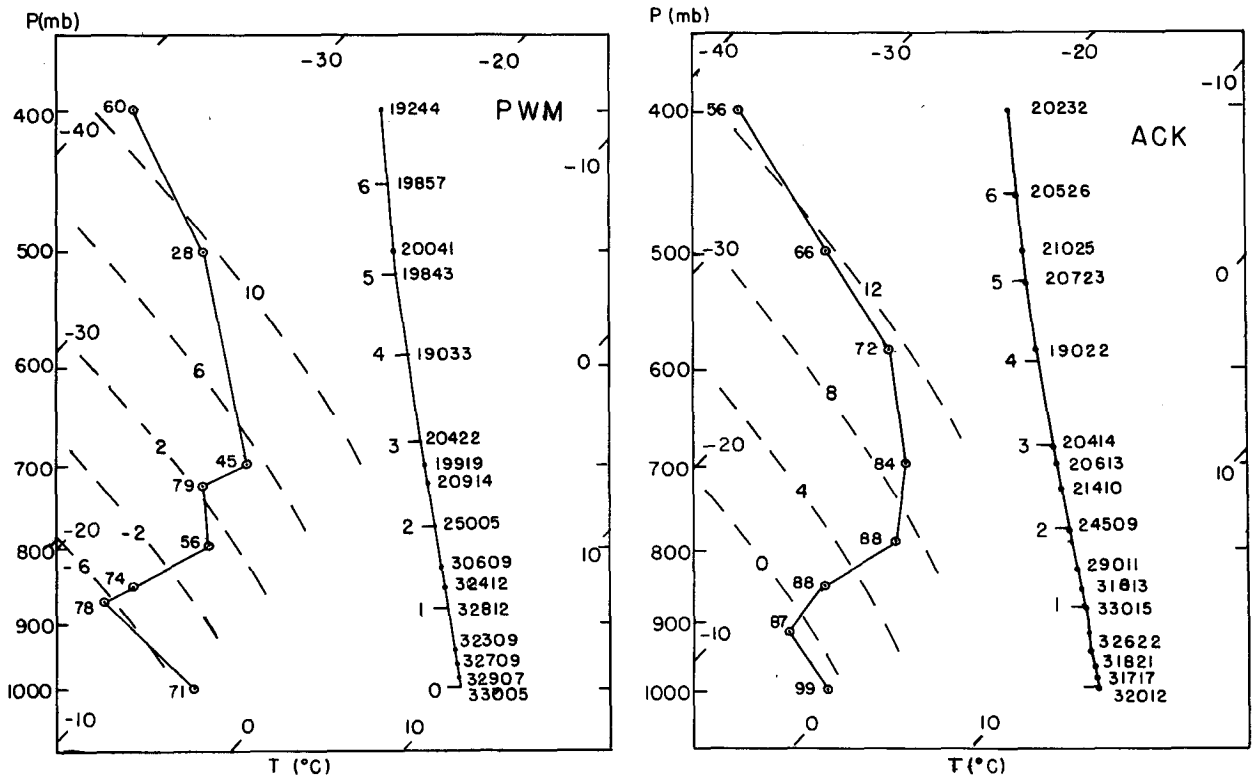

FIG. 9. Soundings at indicated stations, for 1200 UTC 30 December 1962, plotted on Skew T–Log P diagrams. Line to the left indicates temperature profile with pressure. Relative humidity (%) is shown to left of each data point. Line to the right shows height profile with pressure. Elevation (km) is indicated to the left and wind velocity to the right. Direction is given in the first 3 digits and speed (m s^{-1}) in the last two. Dashed lines are reference saturation adiabats, labeled according to the wet-bulb potential temperature (°C).

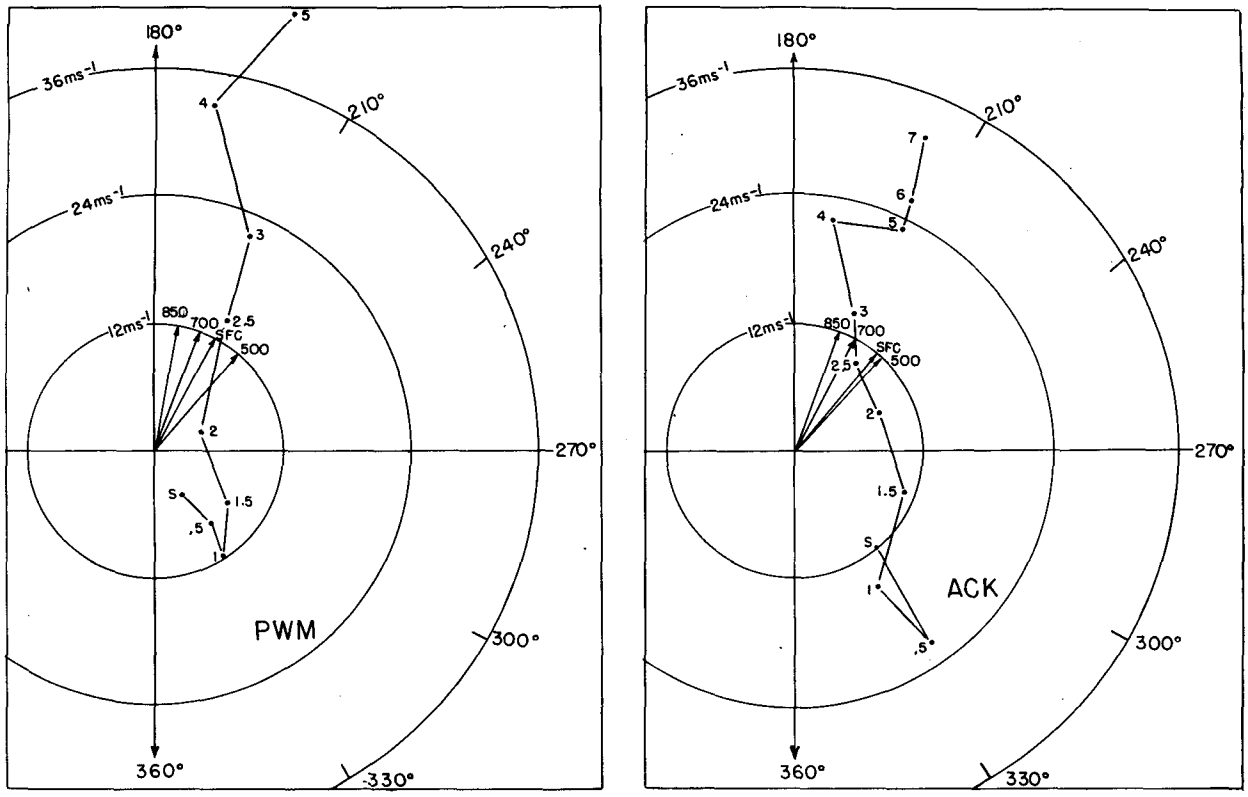

FIG. 10. Hodograms for the indicated stations, at 1200 UTC 30 December 1962. Elevation (km) is indicated by the number adjacent to the data point except for the surface (*S*). The arrows emanating from the origin represent the direction of the geostrophic wind at the indicated levels.

lations for each value. The horizontal decay scale, b^* is estimated as a rough average from the cross section to be 3.1×10^{-6} m^{-1} and the vertical height, H, is taken as 5 km. The stability, expressed as N, the Brunt–Väisälä frequency, is estimated as 1.5×10^{-3} s^{-1} in the sinking colder air, and the symmetric stability is assumed to be vanishingly small in the rising warmer air.

The Emanuel (1985) model then gives as a maximum value of u_{ag} at the surface, 53.7 and 9.25 m s^{-1}, respectively, for the 1000- and 500-mb values of the forcing. The former value can be compared with the value of 66 m s^{-1} obtained from the simple theory discussed previously. Both of these calculated values are much smaller than the estimated observed value at ACK, which is not far from the location of maximum forcing.

The disagreement between theory and observation is due in part to neglect of surface friction, which is surely important in the boundary layer. Even aside from this consideration, however, the semigeostrophic theory is quantitatively reliable only when (in our terms) $[(\delta u_g/\delta M_g)/f]^2 < 1$. In our case, the maximum value of this quantity at 1000 mb is about 4 at this time, at the beginning of the frontal strengthening culminating in the events at Grand Manan. The central implication of semigeostrophic theory is that the component of wind along the isotherms remains in thermal-wind balance during the frontogenetical process. Examination of the vertical shear of the observed wind in Fig. 11, however, shows that it is weaker through the frontal layer than its geostrophic counterpart. (Note that the vertical shear of M_g is the same as that of v_g.) Evidently the development of vertical shear lags behind the development of thermal-wind shear when the forcing is sufficiently intense.

It seems that the situation is comparable to the position in quasi-geostrophic theory, where quantitative reliability cannot be demonstrated for any cyclone which is sufficiently intense to be of more than casual interest. Conceptually, however, the theory in both instances seems useful.

Our results can be compared with numerical calculations from idealized initial conditions. Thorpe and Emanuel (1985), in a semigeostrophic calculation with small symmetric stability in the warm air, show the development of a concentrated front near the ground, but with maximum values of u_{ag} of only about 6 m s^{-1}. Maximum forcing developed near the ground as well, as indicated in our case, although the geostrophic deformation was not allowed to change with time,

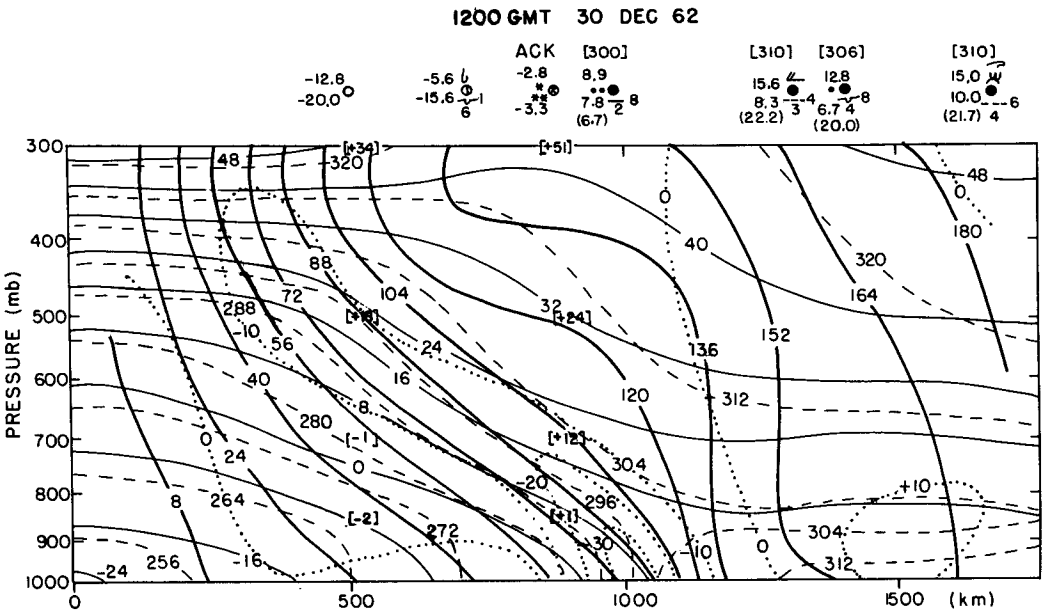

FIG. 11. Vertical cross section for 1200 UTC 30 December 1962 along line shown in Fig. 4. Thin solid lines are potential isotherms, θ, at intervals of 4°C. Thin dashed lines are isotherms of saturation equivalent-potential temperature, at intervals of 8 K. Heavy solid lines are isotachs of $M_g = v_g + fn$ (m s^{-1}), the component of geostrophic absolute momentum normal to the section. The value of (constant) f is 9.446×10^{-5} s^{-1} and the origin of the n-axis is at the left end of the section line. The numbers in brackets within the diagram are the normal components of the observed winds at ACK and at Albany to the northwest. The dotted lines are isopleths of δu_g (m s^{-1}) measured at constant pressure over an interval of 200 km in the n-direction (toward the right along the cross section). Along the top of the diagram are surface observations from ACK and other stations along or near the section line. The elements include sky condition, types, amounts and bases of cloud layers, present weather, temperature, dewpoint and sea surface temperature (in parentheses). The plotting model is conventional. The number in brackets above each marine surface observation is the actual equivalent-potential temperature.

contrary to our case. Their model was inviscid, moreover, but showed forcing between 1 and 2 orders of magnitude smaller than ours.

A more elaborate two-dimensional primitive-equation calculation with detailed boundary-layer physics, according to Keyser and Anthes (1982), yielded a maximum u_{ag} of no more than about 10 m s^{-1}, but on the other hand their forcing appeared likewise much weaker than ours.

The third dimension may have been important in this case. It is clear from Fig. 6 that the cross-front geostrophic component evolved in time and varied in the along-front direction. The implied temporal evolution of the along-front variation of the geostrophic deformation field can be taken into account satisfactorily only in a three-dimensional calculation. It is not clear, however, how such a calculation would be conceptually gratifying except in its confirmation of the validity of Newton's Second Law!

6. Concluding summary

On 30 December 1962, the island of Grand Manan, in the Bay of Fundy, was simultaneously approached by an intensifying cold front from the northwest at the leading edge of a bitterly cold air mass over the continent and by a small explosively intensifying cyclone from the southeast, producing a relatively mild southeasterly gale with rain at the island. Surprisingly, the cold front arrived first, having advanced over the preceding 9 hours against a geostrophic flow increasing from a few meters per second to about 40 m s^{-1}. The mild air returned to a site near the southeast corner of the island, and also at a smaller island a few km to the south, for 1 or 2 h, prior to the passage of the cyclone and the final arrival of the mass of cold air.

The anomalous advance of the cold air in the path of the cyclone was examined by calculating the rate of frontogenesis at the surface attributable to the geostrophic flow. Maximum values of this rate increased from about 100 K (100 km)$^{-1}$ (10^5 s)$^{-1}$ to several times that value along the developing front as the cyclone approached. An overly simplified theory linking the cross-front ageostrophic motion to this geostrophic frontogenesis suggests that 100 of the above units of forcing would correspond to 50 m s^{-1} of ageostrophic motion, on the assumption of inviscid flow with no stratification and a layer of forcing about 3 km deep. Comparison with more accurate theoretical formulations confirms that the simple model overestimates the

ageostrophic response but supports the conclusion that the anomalous frontal behavior was the consequence of geostrophic forcing acting on an already intense horizontal temperature gradient, exacerbated by the coincidental approach of an intense cyclone. Semigeostrophic theory appears to be quantitatively unreliable for even the relatively modest geostrophic forcing present at the beginning of this episode.

Acknowledgments. The authors wish to thank Kerry Emanuel, Massachusetts Institute of Technology (MIT) for discussion and carrying out of the semigeostrophic calculation, and Myhron Tate of Ingalls Head for operating and caring for the Kent Island thermograph, without which the entire account might have been perceived as a result of holiday excess. We are grateful to Isabelle Kole for drafting the figures, to the National Weather Service and the Atmospheric Environment Service for providing crucial data and to the MIT Center for Meteorology and Physical Oceanography for the provision of facilities. One of the authors (F.S.) was supported by the National Science Foundation under Grant ATM-8600543.

REFERENCES

Eliassen, A., 1959: On the formation of fronts in the atmosphere. *The Atmosphere and the Sea in Motion,* B. Bolin, Ed., Rockefeller Institute Press, 277–287.

Emanuel, K., 1985: Frontal circulations in the presence of small moist symmetric stability. *J. Atmos. Sci.,* **42,** 1062–1071.

Hoskins, B. J., and F. P. Bretherton, 1972: Atmospheric frontogenesis models: Mathematical formulation and solution. *J. Atmos. Sci.,* **29,** 11–37.

Keyser, D., and R. A. Anthes, 1982: The influence of planetary boundary layer physics on frontal structure in the Hoskins–Bretherton horizontal shear model. *J. Atmos. Sci.,* **39,** 1783–1802.

Roebber, P. J., 1984: Statistical analysis and updated climatology of explosive cyclones. *Mon. Wea. Rev.,* **112,** 1577–1589.

Sanders, F., 1986: Frontogenesis and symmetric instability in a major New England snowstorm. *Mon. Wea. Rev.,* **114,** 1847–1862.

Sawyer, J. S., 1956: The vertical circulation at meteorological fronts and its relation to frontogenesis. *Proc. Roy. Soc. London,* **A234,** 346–362.

Thorpe, A. J., 1985: The cold front of 13 January 1983. *Weather,* **40,** 34–42.

——, and K. A. Emanuel, 1985: Frontogenesis in the presence of small stability to slantwise convection. *J. Atmos. Sci.,* **42,** 1809–1824.